C-2v-Symmetric C-60 Isomer in the Gas Phase: Experimental Evidence against Buckminsterfullerene (I-h-C-60)

C_{2v}-Symmetric C_{60} Isomer in the Gas Phase: Experimental Evidence against Buckminsterfullerene (I_h-C_{60})

Rui-Ting Chen, Sheng-Jun Zhou, Hua Liang, Zhuo-Zhen Qian, Jian-Mei Li, Qiao He, Lei Zhang, Yuan-Zhi Tan, Xiao Han, Zhao-Jiang Liao, Wei-Zheng Weng, Su-Yuan Xie,* Rong-Bin Huang, and Lan-Sun Zheng

State Key Laboratory for Physical Chemistry of Solid Surfaces and Department of Chemistry, College of Chemistry and Chemical Engineering, Xiamen University, Xiamen, 361005, China

Received: March 16, 2009; Revised Manuscript Received: June 24, 2009

Pure non-IPR (isolated-pentagon-rule) C_{60} isomer has rarely been investigated experimentally. The recently reported availability of $^{\#1809}C_{60}Cl_8$ opens an avenue for experimental investigation of $^{\#1809}C_{60}$, a C_{2v}-symmetric C_{60} isomer having two pairs of fused pentagons. Herein, the experiments on $^{\#1809}C_{60}$ were performed on the basis of thermal dechlorination of $^{\#1809}C_{60}Cl_8$ in the solid state and gas phase. $^{\#1812}C_{60}Cl_6$ was employed for comparative study. As determined by Raman and other methods, $^{\#1809}C_{60}$ from thermal decomposition of $^{\#1809}C_{60}Cl_8$ crystals readily coalesces to form carbon solid with a collapsed crystal lattice. In contrast, dechlorination via thermal spray of $^{\#1809}C_{60}Cl_8$ in the gas phase is feasible for investigation of monodispersed all-carbon C_{60} isomer, because the existence of $^{\#1809}C_{60}$ in the gas phase has been confirmed by experimental evidence from mass spectrometry and high-performance-liquid-chromatography.

Introduction

Although C_{60} has a total of 1812 isomers, buckminsterfullerene $^{\#1812}C_{60}$ (the nomenclature is specified with a spiral algorithm[1]) is the only C_{60} obeying the famous isolated pentagon rule (IPR).[2] All the other C_{60} isomers violate IPR and, thus, render their chemically reactive properties and, in turn, are hard to synthesize in the forms of the pure, all-carbon molecule. For this reason, fullerene research has overwhelmingly depended on $^{\#1812}C_{60}$, for it is the only C_{60} isomer experimentally available.[3] Although more than 20 years have elapsed since the original discovery of buckminsterfullerene,[4] no C_{60} isomer other than $^{\#1812}C_{60}$ was isolated and identified until recently. Two non-IPR C_{60} isomers have now been synthesized as chlorofullerenes, $^{\#1809}C_{60}Cl_8$ and $^{\#1804}C_{60}Cl_{12}$,[5] from the classical Krätschmer–Huffman synthesis[3] introducing CCl_4 as the chlorine source. The structures of these two IPR-breaking chlorofullerenes have been identified by X-ray crystallography.

From the point of structure, $^{\#1809}C_{60}$ and $^{\#1804}C_{60}$ can be transferred to the elegant I_h-symmetric $^{\#1812}C_{60}$ by one or two C–C bond 90° rotations, which is well-known as the Stone–Wales (SW) transformation.[6] Sequentially, C_{60} isomers were considered as reactive intermediates toward buckminsterfullerene in the SW annealing mechanism for fullerene formation.[7–9] Some plausible evidence for the existence of a C_{60} isomer mixture was previously shown in gas phase experiments.[10–12] Due to the similarity of these isomers, however, the structures of isomeric C_{60} intermediates are hard to identify directly in the gas phase. The recent availability of the chlorofullerenes of non-IPR C_{60} isomers[5] provides the possibility for experimental investigation of pure, all-carbon C_{60} isomers other than $^{\#1812}C_{60}$.

$^{\#1809}C_{60}$ has the lowest energy next to $^{\#1812}C_{60}$ among non-IPR C_{60} isomers; it is about 1.6–1.7 eV less stable than $^{\#1812}C_{60}$.[13] The energy difference between these two isomers is only 0.03 eV per atom, Similar to the difference in cohesive energy between diamond and graphite,[14] this energy difference cannot exclude the existence of $^{\#1809}C_{60}$. For experiment, therefore, it may be feasible to investigate this $^{\#1809}C_{60}$ in the form of a pure, all-carbon cluster. However, experimental trial on bare, non-IPR C_{60} isomers is scarce.[10–12,15] Here, we report some experimental evidence to establish the existence of $^{\#1809}C_{60}$, starting from the $^{\#1809}C_{60}Cl_8$ precursor through thermal dechlorination under an inert gas atmosphere. As a typical I_h-C_{60} chloride, $^{\#1812}C_{60}Cl_6$ was employed for contrastive experiment.

Experimental Methods

Synthesis and Isolation. The synthesis of $^{\#1809}C_{60}Cl_8$-containing soot was conducted in a modified Krätschmer–Huffman generator through introducing CCl_4 into the buffer gas. The generator and procedure for the synthesis have been reported previously.[16,17] The soot was extracted by toluene in a supersonic bath and followed by separation with multistep high performance liquid chromatography (HPLC). Preparative isolation was conducted on a LC908W-C60 HPLC instrument (Japan Analytical Industry Co. Ltd.) with a Buckyprep column (250 × 10 mm, Cosmosil Co.). Eluted with toluene at a flow of 1.9 mL/min under 43 °C temperature, the component with a retention time around 19.5 min was purified through multistage recyclic HPLC separation to obtain pure $^{\#1809}C_{60}Cl_8$. Furthermore, $^{\#1812}C_{60}Cl_6$ was synthesized according to the literature[18] and then purified on an Agilent 1200 series HPLC instrument using a Buckyprep column (250 × 4.6 mm, Cosmosil Co.) eluted with 1.0 mL/min toluene at room temperature. The component with retention time of 10.2 min was collected to give pure $^{\#1812}C_{60}Cl_6$. About 2 mg of $^{\#1809}C_{60}Cl_8$ and 2 mg of $^{\#1812}C_{60}Cl_6$ were used for the following experiments.

Raman Spectra. Raman spectra were recorded on a Renishaw 1000 Raman spectrometer in situ during the annealing of a $^{\#1809}C_{60}Cl_8$ single crystal (0.3 mm × 0.2 mm × 1 mm) under argon flow. The setup for the in situ Raman experiment is the same as previously reported.[19] The samples were excited by a laser of 785 nm at a power level of 0.3 mW. The

* Corresponding author. Phone: +86-592-2182151. Fax: +86-592-2183047. E-mail: syxie@xmu.edu.cn.

10.1021/jp902325w CCC: $40.75
Published on Web 09/08/2009

wavelengths were scanned from 100 to 1800 cm^{-1} in 30 s. The annealing temperature was set in a regular interval in the range from room temperature to 500 °C. For recording reliable Raman data at a target temperature, the Ramen experiment was conducted as follows: the sample was annealed to the desired temperature, then the samples were kept at this temperature for 10 min and, finally, cooled down to room temperature for Raman measurement.

Theoretical Calculation for Raman Spectra. To assign the peaks in Raman spectra of $^{\#1809}C_{60}Cl_8$ and $^{\#1809}C_{60}$, we performed first principle calculations using the Gaussian 98 program.[20] The frequencies of $^{\#1809}C_{60}Cl_8$ and $^{\#1809}C_{60}$ were calculated at the B3LYP[21,22]/6-31G* level of theory with the geometry optimized at the same level.

X-ray Diffraction Patterns. X-ray diffraction patterns were recorded on a Bruker CCD Apex-2000 diffractometer using graphite−monochromate Mo Kα (λ = 0.710 73 Å) radiation with a 60 s exposure time. The samples were pretreated in the annealing setup[19] at a temperature of 250 and 500 °C, respectively.

Matrix-Assisted Laser Desorption Ionization Time-of-Flight Mass Spectrometry (MALDI-TOF-MS). MALDI-TOF-MS spectra were acquired on a Bruker Reflex III mass spectrometer. 2,5-Dihydroxybenzoic acid (DHB) was used as the matrix for MALDI-TOF-MS determination. To prepare the sample well-mixed with the matrix, the insoluble sample of 500 °C annealed $^{\#1809}C_{60}Cl_8$ was dispersed in toluene with DHB, and the toluene-soluble sample (i.e., 500 °C annealed $^{\#1812}C_{60}$) was dissolved directly in DHB/toluene solution. Then the toluene-dispersed/dissolved samples were dropped onto sample plates for mass spectrometric analysis. Under a 337 nm wavelength of the laser, the mass spectra were recorded in the positive ion mode (Note that none of the relevant MS signals was observed in the negative mode).

Thermal Spray Experiments. Thermal spray experiments were performed in a Bruker esquire HCT mass spectrometer interfaced by an atmospheric pressure chemical ionization (APCI) source, in which a furnace vaporizer equipped with a spray needle (nebulizer) and a corona needle. Portions of $^{\#1809}C_{60}Cl_8$ (0.861 mg) or $^{\#1812}C_{60}Cl_6$ (0.925 mg) were dissolved in 5.00 mL of toluene to give the sample solution with concentrations of 1.72×10^{-4} and 1.98×10^{-4} mol/L, respectively. The sample solution was injected by a Syringe pump; the methanol was induced as the mobile phase by a HPLC pump. Both the sample solution and the methanol mobile phase were mixed at a T-pattern, three-way valve and flowed into the furnace vaporizer through the spray needle with N_2 as the nebulizer gas. The furnace temperature and flow velocity of the syringe pump can be changed so as to adjust the thermal spray temperature and sample amount supplied. Mass spectrometric conditions were as follows: nebulizer gas, 20 psi; dry gas, 3.0 mL/min; dry temperature, 250 °C; velocity of mobile phase, 0.3 mL/min. The mass spectra were recorded in the negative ion mode because no relevant MS signal was observed in the positive mode. Thermal spray products were also allowed for collection in a cooling toluene trap. The toluene-trapped products were further analyzed by HPLC−MS with a C18 column (250 × 4.6 mm, Supelco Co). In the replacement of widely used HPLC solvent methanol, toluene was used to prevent the resultant thermal spray products from further reaction with methanol.

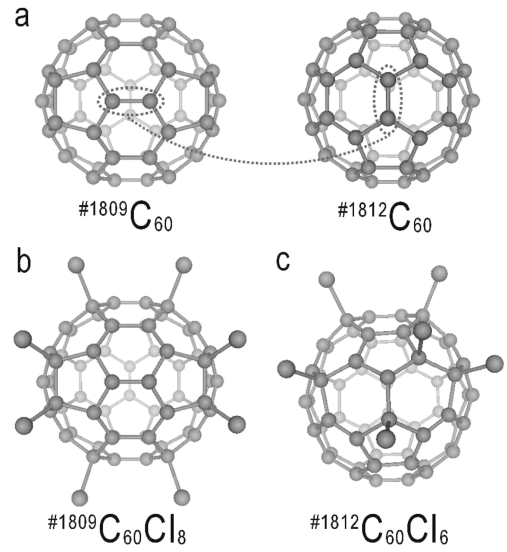

Figure 1. Molecular structures. (a) $^{\#1809}C_{60}$ and $^{\#1812}C_{60}$. Corresponding C−C bonds of Stone−Wales transformation via the 90° rotation are labeled in dashed lines. (b) $^{\#1809}C_{60}Cl_8$. (c) $^{\#1812}C_{60}Cl_6$.

Results and Discussion

Molecular Structures and Stabilities of C_{60} Isomers ($^{\#1809}C_{60}$ and $^{\#1812}C_{60}$) and Their Chloro Derivatives. The structures of $^{\#1809}C_{60}$ and $^{\#1812}C_{60}$ can be transferred to each other by a single SW operation via a 90° rotation of the hexagon−hexagon edge[23] (Figure 1a). $^{\#1809}C_{60}$ is a special species in the SW annealing mechanism for fullerene formation, because 1708 C_{60} isomers transfer toward buckminsterfullerene ($^{\#1812}C_{60}$) through $^{\#1809}C_{60}$.[23] Accordingly, $^{\#1809}C_{60}$ is the only bridge to link the most stable $^{\#1812}C_{60}$ and 94% of the other C_{60} isomers.

Unlike all the pentagons' being separated by hexagons in the I_h-$^{\#1812}C_{60}$ molecule, there are two pairs of fused pentagons on the cage framework of $^{\#1809}C_{60}$. This geometric feature of fused pentagons leads to both higher strain and lower aromaticity for $^{\#1809}C_{60}$. Computation-optimized geometries have shown the π-orbital axis vector (POAV) angle[24] for the carbon at the pentagon fusion of $^{\#1809}C_{60}$ is 15.00°, about 3.4° larger than that of $^{\#1812}C_{60}$ (11.64°). Such a larger POAV angle leads to higher reactivity of the non-IPR C_{60} isomer. To capture the isomeric C_{60} cage, exohedral derivatization has been adopted to stabilize the $^{\#1809}C_{60}$ as $^{\#1809}C_{60}Cl_8$ in the carbon plasma. Shown in Figure 1b is the molecular structure of $^{\#1809}C_{60}Cl_8$. The overall symmetry of $^{\#1809}C_{60}Cl_8$ is C_{2v}, the same as its parent fullerene cage. The chlorine-bonded sp^3-carbon atoms split the cage into two aromatic regions, C_{10} and C_{42}. The larger portions of C_{42} are similar to I_h-C_{60} with alternating C=C and C−C bonds, while the smaller moieties of C_{10} structurally resemble the naphthalene patches.[5] All the carbon atoms at the pentagon fusions are saturated by four chlorine atoms, and in turn, the fused-pentagon-related strains are relieved due to the transformation of carbon hybridation state from sp^2 to sp^3. The other four chlorine atoms are linked at the hexagon−hexagon−pentagon vertexes to satisfy the aromaticity. Therefore, the stability of the non-IPR isomeric C_{60} can be explained by both the "strain relief rule" and "local aromaticity rule".[25] The eight chlorine atoms in $^{\#1809}C_{60}Cl_8$ can be classified into two groups: four locate in pentagon-pentagon fusion sites (Cl_{pp}) and the others locate in the corresponding hexagon−hexagon vertex (Cl_{hh}). The average bond lengths of C−Cl_{pp} and C−Cl_{hh} are 1.77 and 1.81 Å, respectively, likely implying the higher reactivity of C−Cl_{hh}, as demonstrated in the Friedel−Crafts substitution reaction involving $^{\#1809}C_{60}Cl_8$ and benzene.[5]

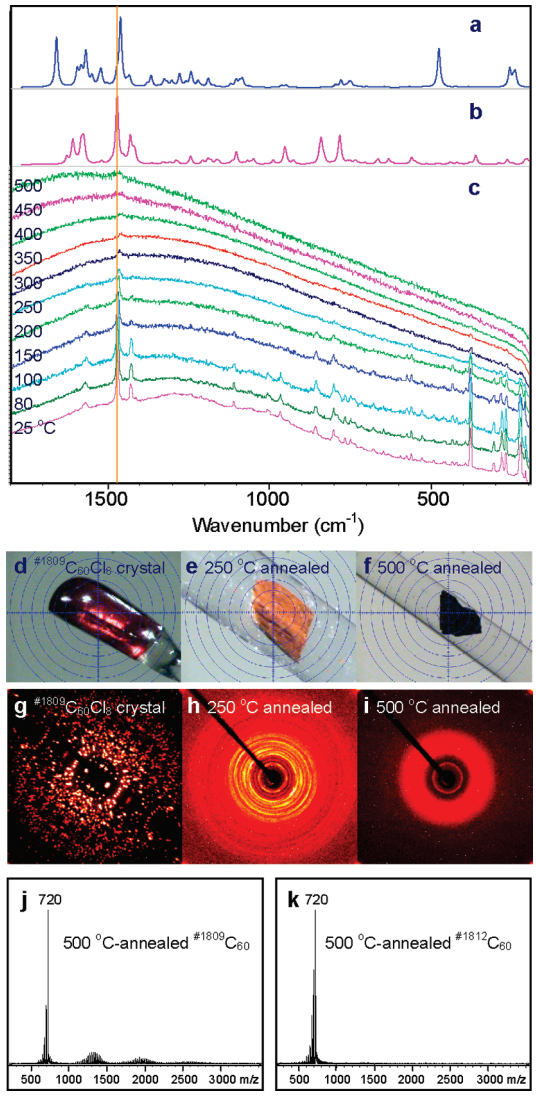

Figure 2. Annealing of the $^{\#1809}C_{60}Cl_8$ species recorded by Raman, X-ray diffraction, and MALDI-TOF-MS. (a, b), Simulated Raman spectra of $^{\#1809}C_{60}$ (a) and $^{\#1809}C_{60}$ Cl_8 (b), scaled by a factor of 0.98. (c) Raman spectra of $^{\#1809}C_{60}Cl_8$ in changing with annealing temperature. (d−f) Morphologic pictures of a $^{\#1809}C_{60}Cl_8$ single-crystal (d), 250 °C-annealed-$^{\#1809}C_{60}Cl_8$ (e), and 500 °C-annealed-$^{\#1809}C_{60}Cl_8$ (f) taken on an optical microscope. (g−i), Corresponding X-ray diffraction patterns. (j, k), MALDI-TOF-MS of 500 °C-annealed $^{\#1809}C_{60}Cl_8$ (j) and 500 °C-annealed $^{\#1812}C_{60}$ (k).

For comparative study, in contrast to $^{\#1809}C_{60}Cl_8$, $^{\#1812}C_{60}Cl_8$ is an ideal species having a predicted derivatization pattern similar to the well-identified structure of $C_{60}Br_8$.[26,27] Unfortunately, $^{\#1812}C_{60}Cl_8$ is experimentally unavailable to date. Therefore, we choose $^{\#1812}C_{60}Cl_6$[28] (Figure 1c), a representative chlorofullerene of $^{\#1812}C_{60}$, for comparative trial. The average C−Cl bond length of $^{\#1812}C_{60}Cl_6$ is about 1.82 Å,[28] slightly longer than those of $C-Cl_{pp}$ bonds in $^{\#1809}C_{60}Cl_8$ and likely having the implication of less stability. In short, pentagon adjacency results in a less stable bare cage but more stable chlorofullerene.

Isomeric C_{60} in Solid State. To experimentally investigate solid $^{\#1809}C_{60}$ in the form of an all-carbon molecule, we performed an annealing experiment with $^{\#1809}C_{60}Cl_8$ crystals under argon flow from room temperature to 500 °C. The annealing dechlorination products of $^{\#1809}C_{60}$ species were tracked in situ by Raman spectra. At room-temperature, the Raman spectrum of the $^{\#1809}C_{60}Cl_8$ crystal shows intense signals at 1470.5, 377.3, 304.5, 280.2, 267.6, and 222.0 cm^{-1} (Figure 2c and the Supporting Information). For assignment of these Raman signals, theoretically simulated Raman spectra of $^{\#1809}C_{60}Cl_8$ (Figure 2b) and $^{\#1809}C_{60}$ (Figure 2c) itself are plotted, as well (related data are listed in the Supporting Information). The most intensive one at 1470 cm^{-1} can be assigned to the pentagonal pinch mode similar to the $A_g(2)$ mode of $^{\#1812}C_{60}$.[29] The other intense peaks ranging from 300 to 222 cm^{-1} are due to the radial mode of the $^{\#1809}C_{60}$ cage. In addition, some signals of moderate or weak intensities are distributed from 1150 to 500 cm^{-1}. Among them, the peaks at 1009, 1002, 968, 860, and 802 cm^{-1} are characteristic vibrational modes related to the sp^3-hybridized C−Cl moieties (including C−C stretching and C−Cl stretching modes). Upon annealing from room temperature to 500 °C, these peaks decrease gradually and completely disappear after 350 °C, indicating the dissociation of the C−Cl bonds. Due to enhanced luminescence in the solid state, the whole spectrum becomes featureless after annealing at 400 °C. Only a weak peak, assignable to the pentagonal pinch mode in the fullerene cage, is distinguishable at 1460 cm^{-1}. This peak is 10 cm^{-1} shifted from the original 1470 cm^{-1} of $^{\#1809}C_{60}Cl_8$. The evidence about the 10 cm^{-1} wavenumber shift, with the implication of complete dechlorination from $^{\#1809}C_{60}Cl_8$ and the existence of a $^{\#1809}C_{60}$ unit in the solid state, is consistent with the calculated wavenumber shift of the pentagonal pinch mode from $^{\#1809}C_{60}Cl_8$ to $^{\#1809}C_{60}$ (Figures 2a, 2b).

The morphology and color transformation of the $^{\#1809}C_{60}$ species are from transparent wine red crystals (Figure 2d) to opaque yellow polycrystals at 250 °C (Figure 2e), followed by insoluble black solid at 500 °C (Figure 2f). The interlayer distances between neighboring molecular layers that are approximately calculated from the smallest diffraction rings in the X-ray diffraction measurement (Figures 2 g-i) are shortened to 8.6 Å at 250 °C and further to 8.3 Å at 500 °C from the original spacing of 9.7 Å in the $^{\#1809}C_{60}Cl_8$ crystal. This suggests the collapse of the crystal lattice and coalescence of the annealed products.

MALDI-TOF-MS provides more obvious evidence of the coalescence. The mass spectrum of 500 °C-annealed $^{\#1809}C_{60}Cl_8$ (insoluble) comprises molecular ions and their aggregation in the ranges of 1200−1500 and 1800−2200 *m/z* (Figure 2j), markedly different from those observed in parallel 500 °C-annealed $^{\#1812}C_{60}$ (soluble) (Figure 2k). Such a difference in the mass spectra likely indicates that the coalescence of $^{\#1809}C_{60}$ occurs possibly in the solid state. So it should be realized that the $^{\#1809}C_{60}$ molecule is too reactive to be studied in the form of a pure, all-carbon molecule in the solid state unless there are chlorines to quench it.

Isomeric C_{60} in the Gas Phase. To work around the coalescence of $^{\#1809}C_{60}$ in the solid state, dechlorination in the gas phase could be rational due to the reduced possibility of immediate collision among gaseous $^{\#1809}C_{60}$ molecules. We adopted a thermal spray method for dechlorination of $^{\#1809}C_{60}Cl_8$ in the gas phase. Shown in Figure 3a is a schematic diagram of the thermal spray device, in which the solution can be nebulized in a tubular furnace in a temperature ranging from room temperature to 500 °C. The sample solution is introduced into the vaporizer through a spray needle, and nebulizing gas is supplied through a concentric tube surrounding the needle. The strong shear forces generated by the nebulizing gas draw out the sample solution, break it into droplets, and disperse it. The droplets are vaporized, desolvented, heated, and partially decomposed at the setting temperature of the furnace. Passing through the furnace, the sample species are allowed to spray

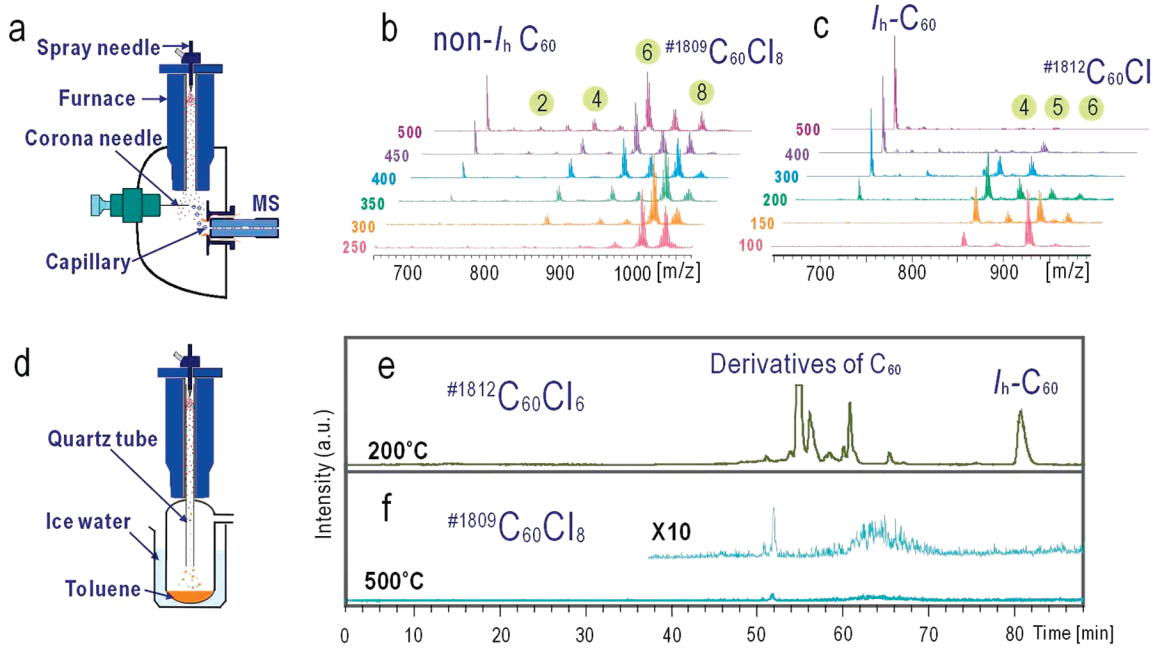

Figure 3. Thermal spray pyrolysis of chlorofullerenes. (a) Schematic diagram of thermal spray parts. (b, c) Mass spectra of $^{\#1809}C_{60}Cl_8$ (b) and $^{\#1812}C_{60}Cl_6$ (c) acquired at different vaporization temperatures. Flow velocity of the syringe pump is 2 μL/min. The intensities of the mass peaks are normalized to the same sum of peak areas of all the fullerene species. (d), Schematic diagram for trapping the thermal dechlorination products. (e, f) HPLC−MS (selected ions monitored at 700−1300 *m/z*) of the toluene-extracted products from spray pyrolysis of $^{\#1812}C_{60}Cl_6$ at 200 °C (e) and $^{\#1809}C_{60}Cl_8$ at 500 °C (f).

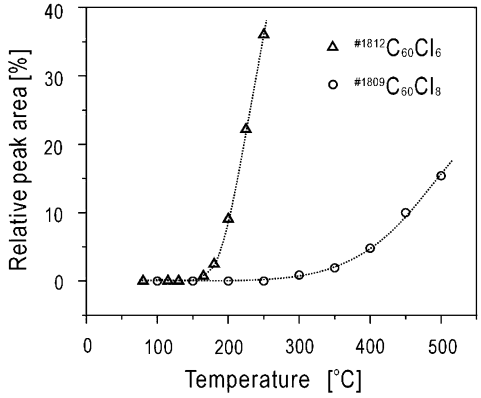

Figure 4. The decomposition curves of $^{\#1809}C_{60}Cl_8$ and $^{\#1812}C_{60}Cl_6$.

onto a corona needle for ionization so as to be detected directly by the mass spectrometer (Figure 3a) or injected into a solvent so as to be collected in solution (Figure 3d). The former is also known as the so-called APCI mass spectrometry.

Figure 3b shows the direct APCI mass spectra of $^{\#1809}C_{60}Cl_8$ in different furnace temperatures ranging from 250 to 500 °C. It is clear that the C−Cl bond breaks down when the temperature increase, and a series of dechlorinated fragments $C_{60}Cl_n$ (n = 0−7) as well as $C_{60}Cl_8(OCH_3)$ from solvolysis reactions are observed. $^{\#1809}C_{60}Cl_8$ lost its chlorines one-by-one and finally formed an all-carbon cage. Further fragmentation was difficult, indicating this C_{60} unit, assignable to $^{\#1809}C_{60}$ (vide infra), can exist in the gas phase.

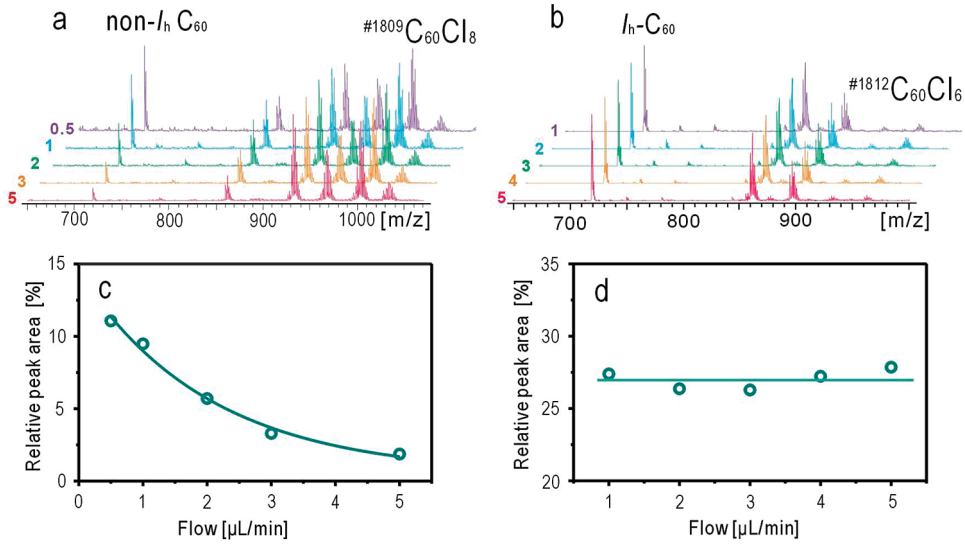

Figure 5. MS and C_{60} relative peak area curves of $^{\#1809}C_{60}Cl_8$ and $^{\#1812}C_{60}Cl_6$ at different concentrations. (a) MS of $^{\#1809}C_{60}Cl_8$ at 400 °C. Flow rates of the syringe pump are 0.5, 1, 2, 3, and 5 μL/min, respectively. (b) MS of $^{\#1812}C_{60}Cl_6$ at 250 °C. Flow rates of the syringe pump are 1, 2, 3, 4, and 5 μL/min, respectively. (c, d) C_{60} relative peak area curves of $^{\#1809}C_{60}Cl_8$ at 400 °C (c) and $^{\#1812}C_{60}Cl_6$ at 250 °C (d).

As a contrastive trial, direct APCI mass spectra of $^{\#1812}C_{60}Cl_6$ from the thermal spray were also recorded in the temperature range of 100−500 °C (Figure 3c). The bare I_h-C_{60} signal is shown after the thermal spray, but the temperature for thermal dechlorination is lower than that of $^{\#1809}C_{60}Cl_8$. To semiquantitatively determine the dechlorination temperature, an approximate method involving the curves of the relative peak area of the resultant C_{60} vs furnace temperature are proposed. The relative peak area of the resultant C_{60} is defined as the MS peak area proportions of C_{60} signal in all corresponding fragments. Due to the slight differences in ionization coefficients in different fullerene species, this peak area ratio is not equal to the percentage of C_{60} concentration in the ion source. However, the C_{60} percentage variation as a function of temperature is useful for checking the decomposition temperature of chlorofullerenes in this system. Figure 4 shows the curves of a C_{60} relative peak area vs the furnace temperature for $^{\#1812}C_{60}Cl_6$ and $^{\#1809}C_{60}Cl_8$, where the inflexions indicate the corresponding decomposition temperature for the formation of a pure, all-carbon cage. Accordingly, the decomposition temperature of $^{\#1809}C_{60}Cl_8$ is about 350 °C. The decomposition temperature of $^{\#1812}C_{60}Cl_6$ is around 180 °C, about 170 °C lower than that of $^{\#1809}C_{60}Cl_8$. The results agree well with the discussion about the geometric implications of the stabilities of the chlorofullerenes, mentioned above.

To assign the structure of C_{60} observed in the thermal dechlorination of $^{\#1809}C_{60}Cl_8$, the spray pyrolysis products were collected in toluene for further HPLC−MS analysis.$^{\#1812}C_{60}Cl_6$ is again employed as the counterpart compound for comparison. In contrast to the remarkable abundance of C_{60} seen in the direct APCI mass spectra of $^{\#1809}C_{60}Cl_8$ at 500 °C (Figure 3b), the signal of the C_{60} unit is missing in the HPLC−MS analysis for the corresponding collected products (Figure 3f). As for $^{\#1812}C_{60}Cl_6$, clear peaks of 720 *m*/*z*, the same as that in the direct mass spectra of $^{\#1812}C_{60}Cl_6$ at 200 °C (Figure 3c), are shown in the HPLC−MS determination (Figure 3e) in which the peak of 720 *m*/*z* can be explicitly assigned to I_h-C_{60} by its HPLC retention time and UV spectrum. According to the obvious difference of HPLC−MS resulting from $^{\#1809}C_{60}Cl_8$ (Figure 3f) and $^{\#1812}C_{60}Cl_6$ (Figure 3e), it is reasonable to assume that these two chlorofullerenes give birth to two classes of C_{60} isomers in the spray pyrolysis process, and the 720 *m*/*z* peak in Figure 3b is due to $^{\#1809}C_{60}$, which is directly derived from $^{\#1809}C_{60}Cl_8$. Because of the highly local curvature and lower stability of non-IPR C_{60} isomer, as mentioned above, it is likely that $^{\#1809}C_{60}$ readily aggregates in the solution to form insoluble species and is therefore undetectable by HPLC−MS.

The existence and the reactivity of $^{\#1809}C_{60}$ in the gas phase were further confirmed by concentration-dependent experiments. Figure 5 shows the APCI mass spectra of $^{\#1809}C_{60}Cl_8$ at 400 °C (Figure 5a) and $^{\#1812}C_{60}Cl_6$ at 250 °C (Figure 5b) in different input amounts, depending on the flow rate of the syringe pump. The relative amount of the resultant C_{60} (720 *m*/*z*) in the mass spectrum of $^{\#1809}C_{60}Cl_8$ decreased markedly from 11 to 2% when the amount of sample increased (Figure 5c), whereas the signal peaks of I_h-C_{60} in $^{\#1812}C_{60}Cl_6$ are shown approximately unchanged (26−28%) for different input amounts (Figure 5d). Although it is well-known that the collision probability increases as the concentration increases, $^{\#1812}C_{60}$ (from the thermal dechlorination of $^{\#1812}C_{60}Cl_6$) with chemical inertness behaves in such a way as to appear to be relatively unaffected by changes in the concentration, even for high concentrations. Due to the reactive properties of $^{\#1809}C_{60}$, however, the increase in collision probability decreased the signals of 720 *m*/*z* significantly.

Conclusion

In conclusion, the existence of isomeric C_{60} is revealed by contrastive experiments on thermal dechlorination of $^{\#1809}C_{60}Cl_8$ and $^{\#1812}C_{60}Cl_6$. The experimental evidence of MS, HPLC, Raman, X-ray diffraction, and MALDI-TOF-MS confirms that $^{\#1809}C_{60}$ exists in the gas phase but readily aggregates in the solid state. The presented evidence demonstrates it is feasible to experimentally investigate pure, all-carbon non-IPR $^{\#1809}C_{60}$ in the future.

Acknowledgment. This work was supported by the National Natural Science Foundation of China (Grants Nos. 20525103, 20531050, and 20721001) and the 973 Program (Grant No. 2007CB815301).

Supporting Information Available: Experimental and simulative Raman spectra of $^{\#1809}C_{60}Cl_8$ and $^{\#1809}C_{60}$. This material is available free of charge via the Internet at http://pubs.acs.org.

References and Notes

(1) Fowler, P. W.; Manolopoulos, D. E. *An Atlas of Fullerenes*; Clarendon Press: Oxford, 1995.
(2) Kroto, H. W. *Nature* **1987**, *329*, 529.
(3) Krätschmer, W.; Lamb, L. D.; Fostiropoulos, K.; Huffman, D. R. *Nature* **1990**, *347*, 354.
(4) Kroto, H. W.; Heath, J. R.; O'Brien, S. C.; Curl, R. F.; Smalley, R. E. *Nature* **1985**, *318*, 162.
(5) Tan, Y. Z.; Liao, Z. J.; Qian, Z. Z.; Chen, R. T.; Wu, X.; Liang, H.; Han, X.; Zhu, F.; Zhou, S. J.; Zheng, Z. P.; Lu, X.; Xie, S. Y.; Huang, R. B.; Zheng, L. S. *Nat. Mater.* **2008**, *7*, 790.
(6) Stone, A. J.; Wales, D. J. *Chem. Phys. Lett.* **1986**, *128*, 501.
(7) Raghavachari, K.; Rohlfing, C. M. *J. Phys. Chem.* **1992**, *96*, 2463.
(8) Eggen, B. R.; Heggie, M. I.; Jungnickel, G.; Latham, C. D.; Jones, R.; Briddon, P. R. *Science* **1996**, *272*, 87.
(9) Mintmire, J. W. *Science* **1996**, *272*, 45.
(10) von Helden, G.; Gotts, N. G.; Bowers, M. T. *Nature* **1993**, *363*, 60.
(11) Yang, S. H.; Pettiette, C. L.; Conceicao, J.; Cheshnovsky, O.; Smalley, R. E. *Chem. Phys. Lett.* **1987**, *139*, 233.
(12) Hunter, J.; Fye, J.; Jarrold, M. F. *Science* **1993**, *260*, 784.
(13) Bettinger, H. F.; Yakobson, B. I.; Scuseria, G. E. *J. Am. Chem. Soc.* **2003**, *125*, 5572.
(14) Yin, M. T.; Cohen, M. L. *Phys. Rev. B* **1984**, *29*, 6996.
(15) Xie, S. Y.; Deng, S. L.; Huang, R. B.; Yu, L. J.; Zheng, L. S. *Chem. Phys. Lett.* **2001**, *343*, 458.
(16) Gao, F.; Xie, S. Y.; Huang, R. B.; Zheng, L. S. *Chem. Commun.* **2003**, 2676.
(17) Gao, F.; Xie, S. Y.; Ma, Z. J.; Feng, Y. Q.; Huang, R. B.; Zheng, L. S. *Carbon* **2004**, *42*, 1959.
(18) Birkett, P. R.; Avent, A. G.; Darwish, A. D. K., H. W.; Taylor, R.; Walton, D. R. M. *J. Chem. Soc., Chem. Commun.* **1993**, 1230.
(19) Weng, W. Z.; Wan, H. L.; Li, J. M.; Cao, Z. X. *Angew. Chem., Int. Ed.* **2004**, *43*, 975.
(20) Frisch, M. J.; et al. *Gaussian 98*; Gaussian, Inc.: Pittsburgh, PA, 1998.
(21) Becke, A. D. *J. Chem. Phys.* **1993**, *98*, 5648.
(22) Lee, C.; Yang, W.; Parr, R. G. *Phys. Rev. B* **1988**, *37*, 785.
(23) Austin, S. J.; Fowler, P. W.; Manolopoulos, D. E.; Zerbetto, F. *Chem. Phys. Lett.* **1995**, *235*, 146.
(24) Haddon, R. C. *Acc. Chem. Res.* **1988**, *21*, 243.
(25) Tan, Y. Z.; Xie, S. Y.; Huang, R. B.; Zheng, L. S. *Nat. Chem.* **2009**, *1*, 450.
(26) Birkett, P. R.; Hitchcock, P. B.; Kroto, H. W.; Taylor, R.; Walton, D. R. M. *Nature* **1992**, *357*, 479.
(27) Troyanov, S. I.; Troshin, P. A.; Boltalina, O. V.; Kemnitz, E. *Fullerenes, Nanotubes, Carbon Nanostruct.* **2003**, *11*, 61.
(28) Shustova, N. B.; Chernyshev, D. Y.; Troyanov, S. I. *Mendeleev Commun.* **2006**, *16*, 209.
(29) Gallagher, S. H.; Armstrong, R. S.; Lay, P. A.; Reed, C. A. *J. Am. Chem. Soc.* **1994**, *116*, 12091.

JP902325W